Current Interruption in Low-Voltage Circuit Breakers

Andrea Balestrero, Luca Ghezzi, Marjan Popov, *Senior Member, IEEE*, and Lou van der Sluis, *Senior Member, IEEE*

***Abstract*—Low-voltage current interruption is studied in this paper in order to develop a suitable blackbox model for low–voltage circuit breakers. The electric arc will be modeled by means of electrical quantities. Accurate post-arc current measurements by a high sensitivity current probe and signal analysis techniques (Savitsky-Golay filtering) are adopted to extract information. A set of interrupting performance evaluators is proposed, and the best performing indicators are selected. Theoretical explanations provide insight in the physical processes of low-voltage interruption. The difference with the classical context of blackbox modeling in medium- and high-voltage circuit breakers is explained, based on the different relative weight of the arc voltage and voltage supply.**

***Index Terms*—Blackbox models, interruption performance evaluators, low-voltage arc, Savitsky–Golay filter.**

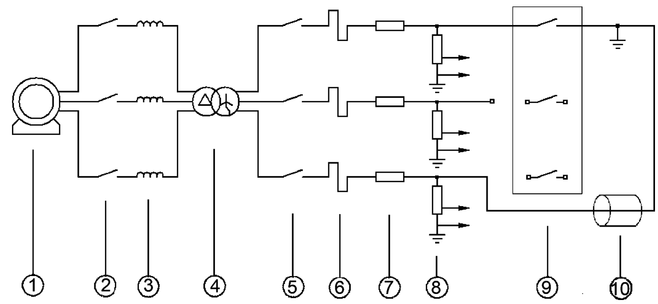

Fig. 1. Scheme of the test network: (1) three-phase generator, (2) backup circuit breaker, (3) air core reactors, (4) three-phase transformers, (5) short-circuit making switch, (6) noninductive shunts for current measurement, (7) resistors, (8) dividers for voltage measurement, (9) breaker under test (one pole tested separately), (10) post-arc current sensor.

I. Introduction

LOW- VOLTAGE (LV) circuit breakers provide protection for circuit ratings of 1000 V or lower. Present day applications are mainly found in residential electric distribution panels, industrial power supply centers and in main power supply panels in large buildings like offices, hospitals and shopping centers. The current interruption capabilities of newly developed breakers and their final compliance with the international standards are assessed during experimental tests in the short circuit laboratory. Mathematical models capable of evaluating the interrupting performance are valuable to assist the development engineers in comparing different breakers and evaluating the effects of the changes in the design.

Two main approaches can be followed which are adopted in medium voltage (MV) and high voltage (HV) [1], namely a completely *a priori* multiphysic modeling, starting from breaker's geometry, applied materials and extinguishing medium, or a simpler blackbox model, based only on electrical quantities. The first approach leads to a large set of partial differential equations to be solved numerically, while the second leads to one or few ordinary differential equations. In the latter case, non electrical phenomena are represented by a suitable set of parameters, which can be identified by means of an initial test and used later to simulate the interrupting behavior for other testing and operating conditions.

Manuscript received June 15, 2009. First published December 08, 2009; current version published December 23, 2009. This work was supported by ABB Italy S.p.A.—Automation Products Division. Paper no. TPWRD-00612-2008.

A. Balestrero is with the ABB S.p.A., Bergamo 24123, BG, Italy (e-mail andrea.balestrero@it.abb.com).

L. Ghezzi is with the ABB S.p.A., Vittuone 20010, MI, Italy (e-mail luca.ghezzi@it.abb.com).

M. Popov and L. van der Sluis are with the Delft University of Technology, Faculty of Electrical Engineering, Mathematics and Computer Science, Delft 2628 CD, The Netherlands (e-mail: m.popov@tudelft.nl vanderSluis}@tudelft.nl).

Digital Object Identifier 10.1109/TPWRD.2009.2035298

Motivated by the very limited computational effort required by blackbox models, especially if compared to the multiphysics approach, this research is intended to investigate a possible extension to the LV realm, and to have a simple tool for development engineering. We begin with an empirical analysis of low-voltage interruptions, looking for performance evaluators which are deducible from test oscillograms, but able to discriminate between good and bad interrupting performances. We are also interested in understanding what leads to a successful interruption: is it the local behavior close to current zero or the global one several time constants before the current zero, and also which differences characterize LV from MV and HV.

In this paper, first we introduce in Section II the experimental setup and the tests performed. Then we describe in Section III the employed signal processing techniques and we define in Section IV the mathematical evaluators of the interrupting performance, divided in a macroscopic and a microscopic approach, with reference to the time span considered. Finally, we analyze the results in Section V and draw our conclusions in Section VI.

II. Experimental Setup

The testing network is shown in Fig. 1, where a 50 Hz ac generator supplies a three-phase network with adjustable reactors and resistors. The tests have been carried out using a three-pole circuit breaker, testing one pole separately; as a consequence, only two branches of the network have been used.

Shunts and dividers measure the arc current and the arc voltage during the whole arcing period. The current ranges from zero to several kiloamperes, and for this reason, the resolution of the signal is not high enough to measure post-arc currents, which typically range from zero up to ten or twenty amperes.

To overcome this problem, a measuring device which is able to measure small currents with a high resolution and capable

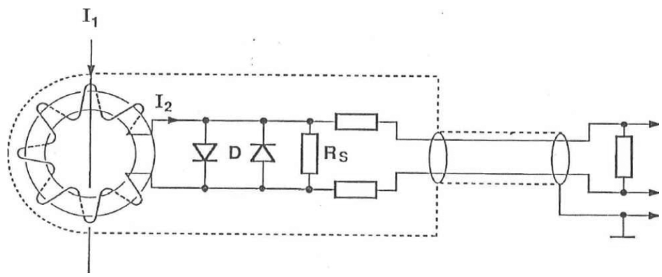

Fig. 2. Basic scheme of the device for post-arc current measurements.

TABLE I
TEST CASES (L/C/R = Left/Central/Right Pole)

Test	Specimen	Pole	Prosp. curr. [kA]	Voltage [V]	Notes
1	1	L	6.0	330	Success
2	1	C	8.0	440	Failure
3	2	L	6.0	330	Success
4	2	R	7.2	400	Success
5	2	C	8.0	440	Success
6	3	L	6.0	330	Success
7	3	C	7.2	400	Success
8	3	R	8.0	440	Failure
9	4	L	7.6	420	Failure
10	4	R	8.4	460	Success
11	4	C	8.8	480	Failure
12	5	L	7.6	420	Success
13	5	C	8.4	460	Success
14	5	R	8.8	480	Success
15	6	C	9.2	500	Failure
16	6	L	9.2	500	Failure
17	6	R	9.2	500	Failure

of withstanding large peak currents has been developed (see Fig. 2). In contrast to commonly used current monitors, saturation of the core of the transformer at high pulses of current is prevented by shunting the turns of the transformer by anti-parallel fast-recovery diodes. The device has a sensitivity of 1 mV/A, is linear within 1% in the range of ±200 A, and is designed for sinusoidal fault currents up to 150 kA. The upper cutoff frequency is 234 kHz.

The sampling rate of the signal from the shunts, from the dividers and from the post-arc sensor is in this test set up 5 MHz, but will in the future be raised to 20 MHz. Voltage and current are measured with a Lecroy Wavesurfer 424 oscilloscope, with a 200 MHz band and 2 Mega points for each channel. Signal sampling is faster than the arc time constant, which is in the order of several tenths of microseconds for air.

All the measurements were carried out with the same impedance, such that a 480 V voltage supply produces a prospective current of 8.7 kA with a $\cos\varphi$ equal to 0.5, in accordance with the UL489 standards for moulded case circuit breakers. The supply voltage has been assigned prescribed values in a range between 300 V and 500 V (see Table I). Since the impedance of the network was kept constant, the current-voltage ratio is also fixed. As a consequence, the current varies accordingly in a range between 6 kA and 9.2 kA.

III. SIGNAL ANALYSIS

Experimental current and voltage time histories need to be suitably postprocessed in order to yield useful information for accurate current zero analysis. The output signals from the shunts and from the post-arc current measuring device have to be merged into a single signal plot, with high currents from the shunts and low currents from the high sensitivity current probe. Since post-arc currents are crucial for the interrupting process, a possible offset has to be removed from the current signal itself.

Noise removal from current and voltage can be accomplished in several ways. First a low pass Gauss filter is applied to damp out high frequency spikes. Given an input sampled time varying signal $\{(x_k, t_k)\}_k$, t being the time, from its discrete FFT spectrum $\{(X_j, f_j)\}_j$, f being the frequency, a new frequency domain spectrum $\{(Y_j, f_j)\}_j$, with $Y_j = X_j \cdot \exp(-f_j^2/B^2)$, is produced and then brought back to the time domain by the inverse discrete FFT. The output sampled temporal signal $\{(y_k, t_k)\}_k$ replaces the original signal, yielding a noise reduction dependent on the cutoff frequency B, which has been set to 100 kHz.

Then, noise removal is further improved by Savitsky-Golay filtering [3], which has the nice property to yield regular time derivatives of the processed signal. The basic idea is to locally approximate data by the least squares fitting polynomial of a specified fixed degree d and computed for a moving window with a specified fixed width, containing an odd number of samples m (the central sample itself and two equally long tails, one before and one after). The fitting polynomial then gives the local value of the smoothed signal and of its derivatives.

We call again $\{(x_k, t_k)\}_k$ the input signal (i.e., the output from the Gauss filter), and assume samples to be equally spaced by a time step h. The following shows how to efficiently deduce the smoothed output signal $\{(y_k, t_k)\}_k$ and its first derivative $\{(t_k, \dot{y}_k)\}_k$. We set $l := (m-1)/2$ and focus on the general kth sample, far away from the edges of the time history, so that a complete window $\{(t_n, x_n)\}_{n=k-l}^{k+l}$ exists, centered on t_k. This is not a major concern, because time histories are usually longer than necessary and may be clipped from their extremities. By means of the affinity

$$t \mapsto z := \frac{(t - t_k)}{h} \tag{1}$$

time is locally linearly rescaled, so that the time window is always mapped, regardless the value of k, to the same subset $\{-l, \ldots, -1, 0, 1, \ldots, +l\}$ of the ring of integers $\mathbb{Z}$ (even though a same t_n will be mapped to different elements of such a set, depending on the relative position inside the moving window, for different values of k).

The least squares fitting polynomial $p_k(z) \in \mathbb{R}[z]$ of a degree not exceeding d, that is,

$$p_k(z) = \sum_{j=0}^{d} a_{k,j} z^j \tag{2}$$

is obtained by solving the set of normal equations. Gathering the $d+1$ unknown polynomial coefficients into vector

$$\mathbf{a}_k = [a_{k,0}, a_{k,1}, a_{k,2}, \ldots, a_{k,d}]^T \tag{3}$$

and the m sample values into vector

$$\mathbf{x}_k = [x_{k-l}, \ldots, x_k, \ldots, x_{k+l}]^T \tag{4}$$

one gets

$$\mathbf{a}_k = (\mathbf{J}^T\mathbf{J})^{-1}\mathbf{J}^T\mathbf{x}_k \tag{5}$$

where the Jacobian matrix $\mathbf{J}$ is such that

$$J_{ij} = (i-l-1)^{j-1},\ i \in \{1,\ldots,m\},\ j \in \{1,\ldots,d+1\}. \tag{6}$$

Thanks to the affinity (1), the matrix $(\mathbf{J}^T\mathbf{J})^{-1}\mathbf{J}^T$ is independent on the particular kth central sample and may thus be computed just only once, with obvious computational advantages.

The Savitsky-Golay method acts as a low pass filter, with a cutting frequency related to the duration of the moving window (the wider the window, the lower the cutting frequency). It is better to keep the degree of the polynomial low (e.g., $d = 3$). The filter may be applied in more than one pass, in order to increase smoothing. One main virtue of the filter is being local, that is, it does not need to operate on the whole set of samples to output one single smoothed sample, unlike, for example, Fourier transform-based filters.

After polynomial (2) is found, the smoothed sample is given by

$$y_k = p_k(0) = a_{k,0} \tag{7}$$

and the time derivative by

$$\dot{y}_k = \frac{d}{dt}p_k(z(t)) = \left.\frac{dp_k}{dz}\right|_{z=0}\frac{dz}{dt} = \frac{a_{k,1}}{h}. \tag{8}$$

Derivatives up to order d may be likewise computed. By induction, the general ℓth derivative $y_k^{(\ell)}$ is readily found to be

$$y_k^{(\ell)} = \ell!\frac{a_{k,\ell}}{h^\ell}, \quad (\ell \le d). \tag{9}$$

The Savitsky–Golay filter is applied to both voltage and current time histories and the time derivative of conductance $g = i/u$ is then suitably computed as

$$\frac{dg}{dt} = \frac{1}{u^2}\left(\frac{di}{dt}u - i\frac{du}{dt}\right). \tag{10}$$

The current zero is the most important and delicate piece of information to be extracted from the oscillograms and thus requires special care. It is identified from the smoothed voltage signal, because its steep descent yields a stable zero point. Linear signal reconstruction in between samples allows a precise zero identification. The smoothed current signal is time shifted to exactly match voltage zero with current zero (see Fig. 3). Time shifting implies signal re-sampling, assuming piecewise linearity, to retain current and voltage values at the same time instants. The conductance is deduced from its definition as the ratio of current over voltage. Close to current zero the ratio becomes undetermined, since both signals vanish, and this causes a spike in the conductance plot. This inessential discontinuity is removed by linear signal reconstruction in between two samples a few microseconds before and after the current zero. The conductance time derivative suffers the same problem and is treated in this way as well.

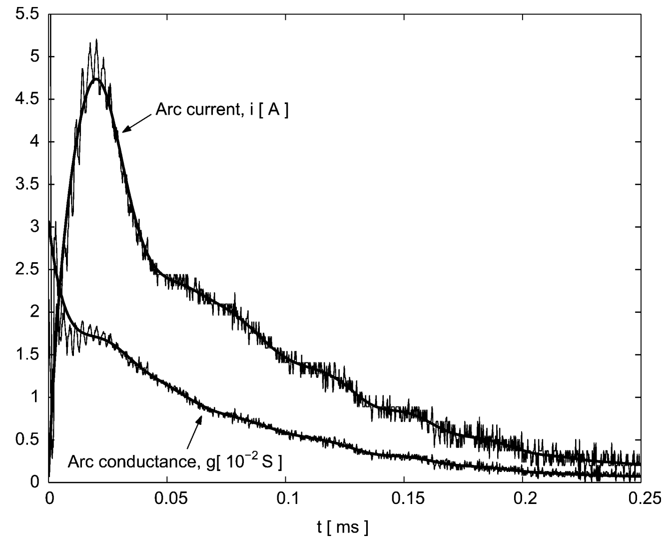

Fig. 3. post-arc current and conductance (bold lines denote filtered signals, thin lines raw signals).

IV. Interruption Evaluators

In order to evaluate the breaker's interrupting performance, we define a set of evaluators η_k (i.e., non-negative, real valued functionals) to be applied to the time histories of electrical quantities in the vicinity of any current zero.

A. Macroscopic Evaluators

An evaluator will be termed *macroscopic* if it requires the value of one or more quantities over a time span whose amplitude is comparable with half the ac period (i.e., 10 ms). Considering the time period from the beginning of arcing (conventionally set as the origin of the time line) to the first current zero t_0, we define:

1) the arc energy

$$\eta_1 := \int_0^{t_0} u(t)\cdot i(t)\,dt; \tag{11}$$

2) the mean value of the arc current

$$\eta_2 := \frac{1}{t_0}\int_0^{t_0} |i(t)|\,dt; \tag{12}$$

3) the maximum value of the arc current

$$\eta_3 := \max_{t\in[0,t_0]} |i(t)|; \tag{13}$$

4) the mean value of the arc voltage

$$\eta_4 := \frac{1}{t_0}\int_0^{t_0} |u(t)|\,dt; \tag{14}$$

5) the maximum value of the arc voltage

$$\eta_5 := \max_{t\in[0,t_0]} |u(t)|. \tag{15}$$

Standard test lab instrumentation (see item 6 and 8 in Fig. 1) can be used for macroscopic evaluators, because only global

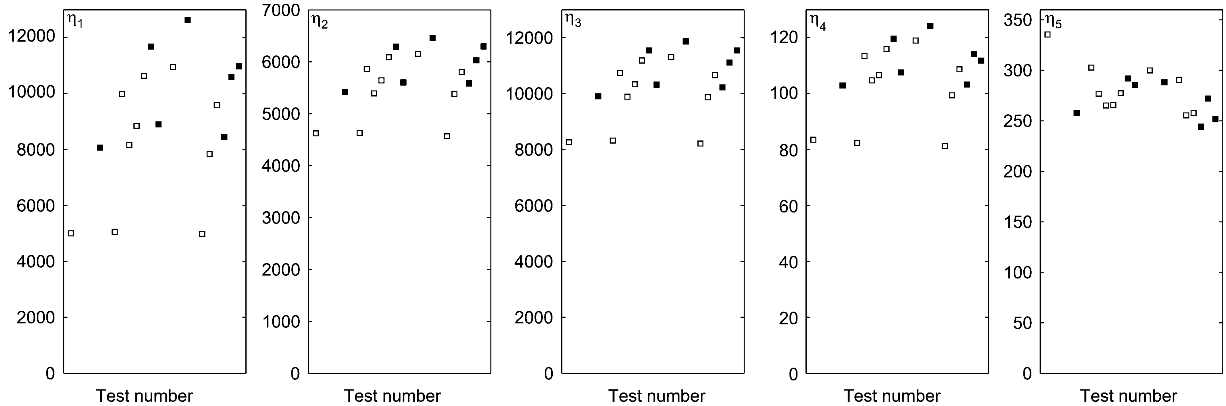

Fig. 4. Macroscopic interruption evaluators. Left to right: arc energy [J], mean arc current [A], max arc current [A], mean arc voltage [V], max arc voltage [V]. White squares denote successes, black denote failures.

time histories are involved and the post-arc region needs not to be recorded in detail. Straightforward signal processing can be applied, a decent noise removal being only required to prevent the max operator from returning a fictitious spike.

B. *Microscopic Evaluators*

An evaluator will be termed *microscopic* if it only requires the value of one or more quantities over a very short time span with reference to the period of ac current, such as hundreds of microseconds, or even a single instant in time. We consider the period close to current zero, since many authors [5]–[7] have shown that this is a suitable area to evaluate the interrupting performance. We use a time span $T = 10\ \mu$s after each current zero and define:

1) the current slope precisely at current zero

$$\eta_6 := \left|\frac{di}{dt}\right|_{t=t_0}; \tag{16}$$

2) the electric charge passing through the post-arc channel over the time interval T

$$\eta_7 := \int_{t_0}^{t_0+T} |i(t)|\, dt; \tag{17}$$

3) the Joule's integral over the time interval T

$$\eta_8 := \int_{t_0}^{t_0+T} i^2(t)\, dt; \tag{18}$$

4) the conductance at current zero

$$\eta_9 := g(t_0); \tag{19}$$

5) the average current slope before current zero

$$\eta_{10} := \frac{|i(t_{10})| - |i(t_{50})|}{t_{10} - t_{50}} \tag{20}$$

where $t_{10} = t_0 - 10\ \mu$s and $t_{50} = t_0 - 50\ \mu$s.

Except for η_{10}, a sensitive current measuring device (see item 10 in Fig. 1) is required for microscopic evaluators, due to small currents in their definition. A good signal processing algorithm, however, is also needed, and Savitsky-Golay method is particularly welcome for η_6, where a precise evaluation of a derivative is also required. In the case of η_7 and η_8, the integral tends to compensate for high frequency fluctuations, so that filtering becomes less important. On the contrary, an accurate zero crossing detection is required for the first four evaluators.

V. Results and Discussion

A. *Macroscopic Evaluators*

Macroscopic evaluators computed from experimental tests are collected in Fig. 4, where white and black squares denote successful interruptions and failures, respectively. Only the first shot on each pole of the breaker is here considered. The testing conditions for each experiment can be found in Table I. The absence of good ordering based on the interruption quality may be clearly observed, so that none of the macroscopic evaluators is able to predict the outcome of the test.

The set of macroscopic indicators does not include the prospective current; as a matter of fact, this indicator turns out to be a rather poor way to predict the outcome of a test: higher prospective currents are more difficult to be interrupted, but a clear threshold can be found only with a great margin of uncertainty.

B. *Microscopic Evaluators*

Microscopic evaluators computed on experimental tests are collected in Fig. 5, where white and black squares denote successful interruptions and failures, respectively. Only the first shot on each pole of the breaker is here considered. In contrast with the macroscopic case, the first four evaluators are a good way to judge the "severity" of a test, because a good ordering can be found with a clear threshold between interruption and failure. This is the essential prerogative every good evaluator should possess.

Starting from this experimental evidence, one may infer that the outcome of the interruption is decided in a neighborhood of the current zero, where the physics of ion recombination dominates. The time constant of these processes is in the order of tenths of microseconds. Therefore, macroscopic evaluators,

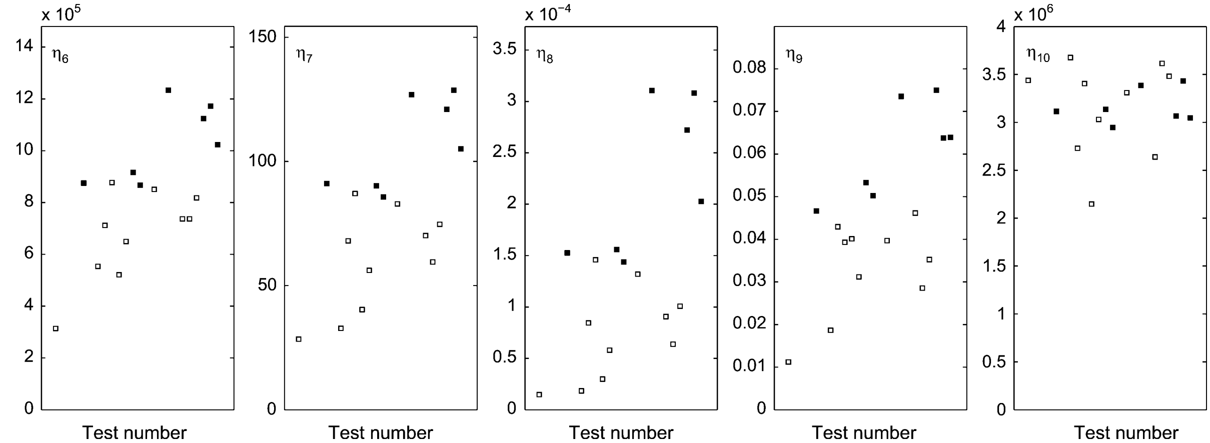

Fig. 5. Microscopic interruption evaluators. Left to right: current slope at CZ [A/s], electric charge through the post-arc channel [C], Joule integral [A^2s], conductance at CZ [S], average current slope before CZ [A/s]. White squares denote successes, black denote failures.

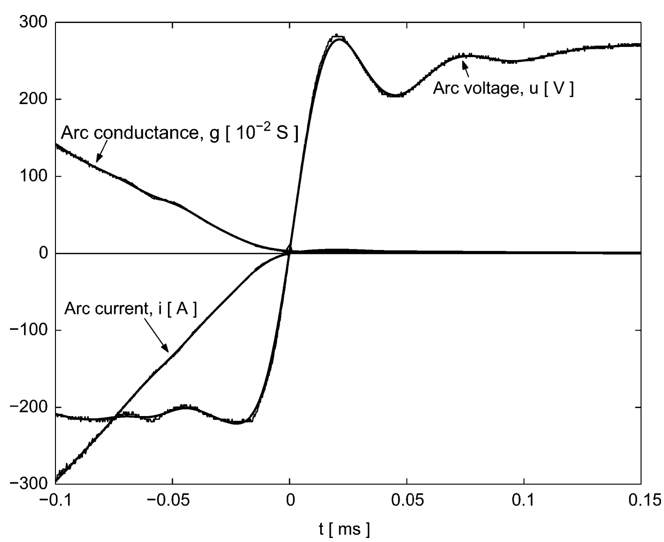

Fig. 6. Arc voltage, arc current and arc conductance in case of a successful interruption.

since based on data apparently too far away from the zone of interest, are not suited to judge the interruption.

Anyway, the past history of the arc should not be neglected, for it provides the initial conditions in the neighborhood of the current zero. The success of microscopic evaluators is due to the implicit presence of these conditions in the relevant portion of the signal analyzed.

Rather surprisingly, the average current slope before current zero seems to be completely unrelated to the interruption performance of the breaker, in contrast with what often has been observed for medium and high voltage breakers [2]. This result is a peculiarity of low-voltage breakers, and can be easily explained with a careful analysis of the interaction between the arc and the supply network.

C. Current Slope Before Current Zero

As can be observed from Fig. 6, the current descent towards current zero may be very well regarded as being linear for the testing conditions. Solving the network equations for a certain instant t^* sufficiently close to current zero (say 50 μs before), so that ohmic voltage drop across the series resistor in the supply circuit becomes negligible, one gets

$$\dot{I}^* \approx \frac{V_s \sin \omega t^* - u^*}{L} \tag{21}$$

where parameters with an asterisk quantities are evaluated at t^*, whilst u^*, I^*, V_s and ω are arc voltage drop, arc current, supply voltage amplitude and radial frequency, respectively. The inductance can be written as

$$L = \frac{V_s \sin \varphi}{\omega I_p} \tag{22}$$

where I_p is the prospective current. If t^* is sufficiently close to the current zero, from (21), we see that the average current slope before zero is related to its value exactly at the zero crossing by

$$\dot{I}^* \approx \dot{I}_0 - \frac{\omega I_p}{\sin \varphi} \frac{u^*}{V_s}. \tag{23}$$

From this equation we deduce that, if $V_s \gg u^*$, then

$$\dot{I}^* \approx \dot{I}_0 \tag{24}$$

so that the two stemming evaluators are equivalent. This is not true in LV realm, where supply and arc voltage are of the same order of magnitude; in other words, there's no reason to expect that the current slope evaluated before current zero and precisely at the current zero carry the same information.

A somewhat deeper insight can be gained from classical blackbox modeling, such as Mayr's one [4], where the arc conductance evolution is described by

$$\frac{1}{g}\frac{dg}{dt} = \frac{1}{\tau_0}\left(\frac{i \cdot u}{P_0} - 1\right) \tag{25}$$

where $i(t)$ and $u(t)$ are the arc current and arc voltage, respectively, related by Ohm's law $g = i/u$, since a perfectly resistive behavior is assumed for the arc. The model has two free parameters: τ_0 (i.e., the arc time constant) and P_0 (i.e., the breaker's cooling power). Taking into account that before the zero crossing the current has a nearly constant slope $\dot{I}^*$, Mayr arc (25) can be solved to obtain the arc voltage. When t^* is chosen to coincide with the latest voltage peak before zero crossing, the relevant u^* can be plugged into the network derived (23). After straightforward manipulations one gets

$$|\dot{I}^*| = \frac{1}{2}\left(|a|I_p + \sqrt{(aI_p)^2 + b\frac{P_0}{\tau_0}\frac{I_p}{V_s}}\right) \qquad (26)$$

where

$$a := \frac{\omega}{\sin\varphi}\sin(\sqrt{2}\omega\tau_0), \quad b := \frac{4\omega}{(2\sqrt{2}+2)\sin\varphi}. \qquad (27)$$

It follows from (26) that an increase of the prospective current I_p increases $\dot{I}^*$, as can be expected since this makes the test more severe. On the other hand, in the spirit of this argumentation the cooling power P_0 acts the opposite way, since a breaker with lower arc quenching properties (lower P_0) would be characterized, *ceteris paribus*, by a lower $\dot{I}^*$. This two counterbalancing effects are typical of LV interruptions, since for large supply voltages the influence of arc parameters vanishes, as becomes evident from taking the limit of (26) for $V_s \to \infty$. This, of course, is another way to say that in MV and HV the current is not influenced by the arc, whilst in LV breakers it definitely is.

VI. Conclusions

After having analyzed the empirical behavior of a LV circuit breaker under typical testing conditions, we have elaborated two sets of mathematical evaluators aimed at discriminating good interruptions from bad ones. The evaluators of the first set, termed macroscopic, are based on electrical data over a relatively large period. Although they can be simply obtained, they are not very useful for evaluating interrupting performances.

This strongly suggests that the fate of interruption is decided in the relatively short period close to current zero and, as a matter of fact, the elements of the second set, which are built accordingly and termed microscopic, do fulfill their task very encouragingly. Unlike in the case of MV and HV breakers, the time derivative of the current before current zero proves to be the only bad microscopic evaluator. The supply voltage and the arc voltage are of the same order of magnitude, so the arc voltage deforms the supply current.

The apparently so precious information hidden in the post-arc region requires a very sensitive measuring device and a careful postprocessing of its signal. We have adopted a high sensitivity current probe and Savitsky-Golay filtering, respectively, obtaining good and stable results. Starting from these conclusions, the next step will be to explore the possibility of blackbox modeling of LV breakers in our future research activities.

References

[1] State of the Art of Circuit-Breaker Modeling, Working Group 13.01 of Study Committee 13. CIGRE.

[2] P. H. Schavemaker and L. van der Sluis, "Quantification of the interrupting performance of high-voltage circuit breakers," *Proc., Inst. Elect. Eng., Sci. Meas. Techol.*, vol. 149, no. 4, pp. 153–157, Jul. 2002.

[3] A. Savitsky and M. Golay, "Smoothing and differentiation of data by simplified least squares procedures," *Anal. Chem.*, vol. 36, pp. 1627–1639, 1964.

[4] O. Mayr, "Beiträge zur Theorie des statischen und des dynamischen Lichtbogens," *Arch. Elektrotech.*, vol. 37, pp. 588–608, 1943.

[5] W. Widl, P. Kirchesch, and W. Egli, "Use of integral arc models in circuit breakers testing and development," *IEEE Trans. Power Del.*, vol. 3, no. 4, pp. 1685–1691, Oct. 1988.

[6] G. Bizjak, P. Zunko, and D. Povh, "Circuit breaker model for digital simulation based on Mayr's and Cassie's differential arc equations," *IEEE Trans. Power Del.*, vol. 10, no. 3, pp. 1310–1315, Jul. 1995.

[7] G. St-Jean, M. Landry, M. Leclerc, and A. Chenier, "A new concept in post-arc analysis applied to power circuit-breakers," *IEEE Trans. Power Del.*, vol. 3, no. 3, pp. 1036–1044, Jul. 1988.

Andrea Balestrero was born in Recco, Italy on July 13, 1980. He received the M.Sc. degree in theoretical physics from the Universitá degli studi di Genova, Genova, Italy, in 2004.

He joined ABB in 2005, where he was involved in the electric arc research and in the development of new simulation techniques for the interrupting process in low-voltage breakers.

Luca Ghezzi was born in Gallarate, Italy, on September 21, 1974. He received the M.Sc. degree in structural civil engineering from the Politecnico di Milano, Milano, Italy, in 1999 and a second M.Sc. degree in mathematics from the University of Milan, Milan, Italy, in 2007.

He joined ABB in 2001 and was involved in the development of computational methods for the virtual simulation of physical phenomena, including coupled nonlinear problems, such as arc plasma. As a mathematician, his interest is for domain decomposition preconditioners for the spectral element method.

Marjan Popov (M'95–SM'03) received the Dipl.-Ing. and M.S. degrees in electrical engineering from the Sts. Cyril and Methodius University in 1993 and 1998, respectively, and the Ph.D. from Delft University of Technology, Delft, The Netherlands, in 2002.

From 1993 until 1998, he was a Teaching and Research Assistant at the University of Skopje, Faculty of Electrical Engineering. In 1997, he was an Academic Visitor at the University of Liverpool, Liverpool, U.K. Currently. he is with the Power System Laboratory at the of TechnolgyTU Delft, in the group of Electrical Power Systems. His major fields of interest are arc modeling, transients in power systems, parameter estimation, and relay protection.

Lou van der Sluis (SM'86) was born in Geervliet, the Netherlands, on July 10, 1950. He received the M.Sc. degree in electrical engineering from the Delft University of Technology, Delft, The Nethlerlands, in 1974.

He joined the KEMA High Power Laboratory in 1977 as a Test Engineer and was involved in the development of a data-acquisition system for the High Power Laboratory, computer calculations of test circuits, and the analysis of test data with a digital computer. In 1990, he became a Part-Time Professor and since 1992, he has been a Full-Time Professor at the Delft University of Technology in the Power Systems Department, Delft, The Netherlands.

Prof. van der Sluis is with CC-03 of CIGRE and CIRED to study the transient recovery voltages in medium- and high-voltage networks.